Pionic decay of a possible d' dibaryon and the short-range NN interaction

I. T. Obukhovsky,[1,2] K. Itonaga,[2,3] Georg Wagner,[2] A. J. Buchmann,[2] and Amand Faessler[2]
[1]*Institute of Nuclear Physics, Moscow State University, 119899 Moscow, Russia*
[2]*Institute for Theoretical Physics, University of Tübingen, Auf der Morgenstelle 14, D-72076 Tübingen, Germany*
[3]*Laboratory of Physics, Miyazaki Medical College Kiyotake, Miyazaki 889-16, Japan*
(Received 15 July 1997)

We study the pionic decay of a possible dibaryon $d' \to N+N+\pi$ in the microscopic quark shell model. The initial d' dibaryon wave function ($J^P=0^-$, $T=0$) consists of one $1\hbar\omega$ six-quark shell-model $s^5p[51]_X$ configuration. The most important final six-quark configurations $s^6[6]_X$, $s^4p^2[42]_X$, and $(s^4p^2-s^52s)[6]_X$ are properly projected onto the NN channel. The final state NN interaction is investigated by means of two phase-equivalent—but off-shell different—potential models. We demonstrate that the decay width $\Gamma_{d'}$ depends strongly on the short-range behavior of the NN wave function. In addition, the width $\Gamma_{d'}$ is very sensitive to the mass and size of the d' dibaryon. For dibaryon masses slightly above the experimentally suggested value $M_{d'}=2.065$ GeV, we obtain a pionic decay width of $\Gamma_{d'}\approx 0.18-0.32$ MeV close to the experimental value $\Gamma_{d'}\approx 0.5$ MeV. [S0556-2813(97)04811-5]

PACS number(s): 14.20.Pt, 13.30.Eg, 13.75.Cs

I. INTRODUCTION

During the last decade much attention has been devoted to theoretical and experimental investigations of the pionic double charge exchange (πDCX) process on nuclei. Because this reaction $\pi^+ + (A,Z) \to (A,Z+2) + \pi^-$ involves (at least) two nucleons in the nucleus, the πDCX cross section depends sensitively on short-range NN correlations in nuclei. Therefore, it provides a good testing ground for the nucleon-nucleon interaction at short range. Experiments on different nuclear targets have unambiguously confirmed the existence of a narrow resonancelike structure in the πDCX cross section at small incident pion energies $T_\pi \approx 50$ MeV [1]. The position of this peak turned out to be largely independent of the studied nucleus. The height and width of this peak could not be explained by standard calculations based on the two-step process [2] ($n+n+\pi^+ \to n+p+\pi^0 \to p+p+\pi^-$). So far, these data could only be explained with the assumption of a non-nucleonic reaction mechanism [1,4] proceeding via an intermediate dibaryon resonance, henceforth called d'. The quantum numbers of the d' dibaryon candidate were determined as $J^P=0^-$, $T=0$, and its free mass and hadronic decay width were suggested to be $M_{d'}=2.065$ GeV and $\Gamma_{d'}\simeq 0.5$ MeV.[1] More than a decade ago Mulders *et al.* [5] predicted a dibaryon resonance with quantum numbers $J^P=0^-$, $T=0$ and a mass $M\approx 2100$ MeV within the MIT bag model. Recently, this dibaryon candidate has been investigatedy in a series of works [6–8] within the Tuebingen chiral constituent quark model. These works emphasize the crucial role of the confinement mechanism for the existence of the d'.

The quantum numbers $J^P=0^-$, $T=0$ of the d' resonance prevent the decay into two nucleons and the only allowed hadronic decay channel of the d' is the three-body decay into a πNN system with S waves in each particle pair [1,4]. Because the d' mass $M_{d'}$ is only ≈ 50 MeV above the πNN threshold, the d' decay width $\Gamma_{d'}$ should be anomalously small owing to a very small phase volume of three-particle final states. We recall that the currently available experimental evidence of dibaryon excitations in nuclei is very limited [9]. This is due to very large N-N decay widths of most dibaryon resonances, which renders them undetectable on the background of other hadronic processes at intermediate energy. At present, the experimental evidence for narrow dibaryons is reduced to a single candidate, the $d'(2065)$. In contrast to the deuteron, which consists of two on the average widely separated nucleons, there are indications [6,7] that the d' is a rather pure compound six-quark system. Therefore, the dynamics of its hadronic decay into the πNN system should be sensitive to the overlap region of the two outgoing nucleons, a situation that is ideal for understanding the role of quark degrees of freedom in the short-range nucleon-nucleon interaction (see, e.g., Ref. [10] and references therein).

Starting from this point (for alternative approaches see in Refs. [2,11,12]) we consider the d' decay as a (quark) shell-model transition from one six-quark configuration to another one by emitting a pion. The quark line diagram of the decay is sketched in Fig. 1. The calculation of the transition matrix elements $d' \to N+N+\pi$ is similar to the calculation of Δ-isobar-decay matrix elements $\Delta \to N+\pi$ (spin and isospin flip of a quark). In the case of the d' decay only the initial dibaryon state is a definite six-quark configuration (the lowest shell-model configuration with quantum numbers $J^P=0^-$, $T=0$), whereas the final state consists of a continuum of NN states which have to be projected onto a basis of six-quark configurations with quantum numbers $J^P=0^+$, $T=1$ of the $NN\ ^1S_0$ wave. The main difficulty in comparing the calculated width $\Gamma_{d'}$ with experimental data is its sharp dependence on the energy gap between $M_{d'}$ and the πNN threshold. A reliable result on $\Gamma_{d'}$ can be obtained only if the

[1]This value is uncertain by a factor of 2 [3].

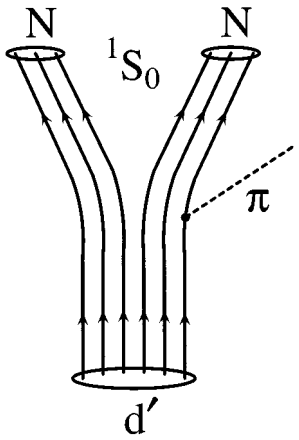

FIG. 1. Quark line diagram of the pionic dibaryon decay. The elementary pion is produced on a single quark, leaving the remaining six quarks in a relative $^1S_0$ nucleon-nucleon scattering state.

exact mass $M_{d'}$ in vacuum is known (e.g., from electroexcitation of the d' on the deuteron at large momentum transfers [13]). At present, we have only indirect data in the nuclear medium [1]. Because of the absence of vacuum data, we investigate the problem of the d' decay width starting from theoretical quark-model results [6,7] for $M_{d'}$ and the hadronic d' size parameter b_6.

Our first calculation for $\Gamma_{d'}$ was published in Ref. [8]. The aim of the present work is to improve mainly on three important effects which were neglected in Ref. [8]: (a) antisymmetrization of the final NN state on the quark level taking into account the effect of quark exchange between the two nucleons at short range, (b) insertion of a complete basis of final six-quark states including besides the nonexcited s^6 shell-model state all Pauli-allowed excited configurations s^4p^2 and s^52s, which have a nonvanishing overlap with the final NN state and can be populated via the emission of the pion from the initial d' dibaryon, and (c) inclusion of the final state interaction (FSI) for the two-nucleon system.

II. DECAY DYNAMICS IN TERMS OF QUARK DEGREES OF FREEDOM

A. Initial state

As in Ref. [8] we consider only the simplest six-quark configuration $s^5p[51]_X$ in the initial state [the energetically lowest $J^P=0^-$, $T=0$ translationally invariant shell-model (TISM) state which satisfies the Pauli exclusion principle]. It has been shown in [6,7] that the d' wave function may be considered as a compound six-quark state, for which a single shell-model vector provides an adequate description. This state vector is defined by

$$|d'\rangle=|s^5p(b_6)[51]_X,\quad [2^3]_C[3^2]_T([2^21^2]_{CT})[42]_S:[21^4]_{CTS},\quad LST=110,\quad J^P=0^-\rangle. \tag{1}$$

The characteristic oscillator parameter in the six-quark wave function b_6 may, for example, be determined from the minimization of the d' mass for a given microscopic quark-quark Hamiltonian [6,7]. The Young schemes $[f_D]$, $D=X,C,S,T$ in orbital, color, spin, and isospin space, as well as for the coupled spaces CT, CTS, are necessary for the unambigious classification of shell-model basis vectors in terms of irreducible representations (IR) of the following reduction chain for unitary groups:

$$\mathrm{SU}(24)_{XCST}\supset \mathrm{SU}(2)_X\times \mathrm{SU}(12)_{CST}\supset \mathrm{SU}(2)_X\times \mathrm{SU}(6)_{CT}$$
$$\times \mathrm{SU}(2)_S\supset \mathrm{SU}(2)_X\times \mathrm{SU}(3)_C\times \mathrm{SU}(2)_T\times \mathrm{SU}(2)_S. \tag{2}$$

The fractional parentage coefficient (FPC) technique [14–17] based on scalar factors (SF's) of Clebsch-Gordan coefficients of the above group [16–19], sketched in the following section, is used for the calculation of matrix elements and overlap integrals.

B. Transition operator

The pionic decay width of the d' is calculated, as in Ref. [8], assuming a direct coupling of constituent quarks with the isotriplet of pion fields $\boldsymbol{\phi}$ through the operator

$$\hat{\mathcal{O}}_{\pi q}(\mathbf{k})=\frac{f_{\pi q}}{m_\pi}\sum_{j=1}^{6}(\boldsymbol{\sigma}_j\cdot\mathbf{k})(\boldsymbol{\tau}_j\cdot\boldsymbol{\phi})\,\frac{\exp[-i\mathbf{k}\cdot(\mathbf{r}_j-\mathbf{R}_{\mathrm{c.m.}})]}{\sqrt{2E_\pi(2\pi)^3}}. \tag{3}$$

Here, $\mathbf{r}_j$, $\boldsymbol{\sigma}_j$, and $\boldsymbol{\tau}_j$ are coordinate, spin, and isospin of the jth quark, $\mathbf{k}$ is the pion momentum in the center-of-mass system (c.m.s.) of the d', and $E_\pi=\sqrt{m_\pi^2+\mathbf{k}^2}$. $f_{\pi q}$ is the πqq coupling constant. Its value is connected with the πNN coupling $f_{\pi N}$ (we use $f_{\pi N}^2/4\pi=0.07491$) through the known relation $\langle N(123)|\Sigma_{j=1}^3\sigma_j^{(z)}\tau_j^{(z)}|N(123)\rangle=\frac{5}{3}\langle N|\sigma_N^{(z)}\tau_N^{(z)}|N\rangle$, giving $f_{\pi q}=\frac{3}{5}f_{\pi N}$. Because we neglect isospin-breaking effects in this work, we chose the average pion mass $m_\pi=138$ MeV.

C. Final states

In Ref. [8] the wave function of the final NN state was antisymmetrized and normalized on the nucleon level, assuming a plane wave with wave vector $\mathbf{q}$ in the relative coordinate $\mathbf{r}$ between the two nucleons. The coordinate representation of the nucleon-nucleon state vector $|\Phi_{NN}(\mathbf{q})\rangle$ was then written as

$$\langle \mathbf{r}|\Phi_{NN}(\mathbf{q})\rangle = \Phi_{NN}(\mathbf{q},\mathbf{r}) = \frac{1}{(2\pi)^{3/2}}\frac{1}{\sqrt{2}} \times [e^{i\mathbf{q}\cdot\mathbf{r}} - (-1)^{(S+T)}e^{-i\mathbf{q}\cdot\mathbf{r}}], \quad S=0, \quad T=1. \tag{4}$$

The full wave function of the final state took into account the three-quark cluster nature of the nucleons

$$\langle \mathbf{r}|\tilde{\Psi}_{NN}(\mathbf{q},123456)\rangle = \Phi_{NN}(\mathbf{q},\mathbf{r})\{N(123)N(456)\}_{ST}; \tag{5}$$

i.e., the nucleon wave function $N(123)$ was given by translationally invariant shell-model (TISM) configurations

$$\begin{aligned} N(123) &= |s^3(b_N)[3]_X, [1^3]_C[21]_T([21]_{CT})[21]_S : [1^3]_{CTS},\ LST=0,1/2,1/2\rangle_{TISM} \\ &= \Phi_N(123)\cdot\ \chi^{C=0}\cdot\chi^{S=1/2}_{S_z}\cdot\chi^{T=1/2}_{T_z}. \end{aligned} \tag{6}$$

$\chi^{C=0}$, $\chi^{S=1/2}_{S_z}$, and $\chi^{T=1/2}_{T_z}$ are color-singlet, spin, and isospin three-quark states. $\Phi_N(123)$ is the orbital part of the wave function, expressed in terms of the internal Jacobi coordinates $\boldsymbol{\rho}=\mathbf{r}_1-\mathbf{r}_2$ and $\boldsymbol{\lambda}=\mathbf{r}_3-(\mathbf{r}_1+\mathbf{r}_2)/2$,

$$\Phi_N(123) = (\sqrt{3}\pi b_N^2)^{-3/2}\exp\left[-\frac{1}{2b_N^2}\left(\frac{1}{2}\rho^2+\frac{2}{3}\lambda^2\right)\right], \tag{7}$$

with a characteristic nucleon oscillator parameter b_N. This parameter does not have to be the same as the harmonic oscillator parameter b_6 for the dibaryon wave function of Eq. (1), as has been discussed in Refs. [6,7]. The relative Jacobi coordinate between the clusters is given by

$$\mathbf{r} = \frac{\mathbf{r}_1+\mathbf{r}_2+\mathbf{r}_3}{3} - \frac{\mathbf{r}_4+\mathbf{r}_5+\mathbf{r}_6}{3}. \tag{8}$$

Note that the six-quark final state (5) is antisymmetrized automatically when the state vector $|\tilde{\Psi}_{NN}(\mathbf{q})\rangle$ is substituted into the decay matrix element $\langle\tilde{\Psi}_{NN}(\mathbf{q});\pi|\hat{\mathcal{O}}_{\pi q}|d'\rangle$, because the initial state of Eq. (1) is fully antisymmetric. However, the antisymmetrizer projector $\hat{\mathcal{A}}$ ($\hat{\mathcal{A}}^2=\hat{\mathcal{A}}$) contained in the initial state $\hat{\mathcal{A}}|d'\rangle=|d'\rangle$ reduces considerably the normalization of the final state [it cuts all nonantisymmetrized parts of the cluster function of Eq. (5) which contain about 90% of the wave function—see below]. Therefore, it is important to substitute from the beginning a final state wave function which is normalized ($\mathcal{N}$) and antisymmetrized ($\hat{\mathcal{A}}$) on the quark level:

$$|\Psi_{NN}(\mathbf{q},123456)\rangle = \mathcal{N}\hat{\mathcal{A}}\{\Phi_{NN}(\mathbf{q},\mathbf{r})N(123)N(456)\}_{ST}, \quad ST=01. \tag{9}$$

The normalization factor $\mathcal{N}$ is determined by the standard orthonormalization condition

$$\langle\Psi_{NN}(\mathbf{q}')|\Psi_{NN}(\mathbf{q})\rangle = \langle\Phi_{NN}(\mathbf{q}')|\Phi_{NN}(\mathbf{q})\rangle = \delta^{(3)}(\mathbf{q}'-\mathbf{q}), \tag{10}$$

which leads to

$$\mathcal{N}^{-2} = \frac{\langle\{\Phi_{NN}(\mathbf{q}')N(123)N(456)\}_{ST}|\hat{\mathcal{A}}|\{\Phi_{NN}(\mathbf{q})N(123)N(456)\}_{ST}\rangle}{\langle\Phi_{NN}(\mathbf{q}')|\Phi_{NN}(\mathbf{q})\rangle}. \tag{11}$$

The antisymmetrizer projector $\hat{\mathcal{A}}$ is

$$\hat{\mathcal{A}} = \frac{3!3!2}{6!}\left(1-\sum_{i=1}^{3}\sum_{j=4}^{6}P_{ij}^{XCST}\right) = \frac{1}{10}(1-9P_{36}^{XCST}), \quad \hat{\mathcal{A}}^2=\hat{\mathcal{A}}. \tag{12}$$

P_{ij}^{XCST} is the pair-permutation operator for quarks i and j in orbital, color, spin, and isospin space. It is instructive to calculate the normalization factor (11) algebraically by factorization of the CST and X parts of the pair permutation $P_{36}^{XCST} = P_{36}^{CST}P_{36}^{X}$. The matrix element of P_{36}^{CST} between two NN states in the $ST=01$ (or 10) channel is very well known (see, e.g., [18]):

$$\langle\{N(123)N(456)\}_{ST=01}|P_{36}^{CST}|\{N(123)N(456)\}_{ST=01}\rangle = -\tfrac{1}{81}. \tag{13}$$

Inserting this value into Eq. (11) reduces its right-hand side to

$$\mathcal{N}^{-2}=\frac{1}{10}+\frac{1}{90}\frac{\langle\Phi_{NN}(\mathbf{q}')\Phi_N(123)\Phi_N(456)|P_{36}^X|\Phi_{NN}(\mathbf{q})\Phi_N(123)\Phi_N(456)\rangle}{\langle\Phi_{NN}(\mathbf{q}')|\Phi_{NN}(\mathbf{q})\rangle}, \tag{14}$$

where $\Phi_N(123)$ is the orbital part of the nucleon wave function (6) given in Eq. (7). The numerator in Eq. (14) depends on the form of $\Phi_{NN}(\mathbf{q},\mathbf{r})$, but for the plane wave in Eq. (4) (or for any continuum wave function including FSI's) it is a finite value: i.e., it has to be zero compared with the δ function in the denominator. Therefore, in our case the second term in Eq. (14) vanishes and we obtain

$$\mathcal{N}=\sqrt{10}. \tag{15}$$

Note that the expression

$$\langle P_{36}^X\rangle\equiv\langle\Phi_{NN}\Phi_N\Phi_N|P_{36}^X|\Phi_{NN}\Phi_N\Phi_N\rangle/\langle\Phi_{NN}|\Phi_{NN}\rangle$$

receives its maximal value$=1$ in the special case of a Gaussian $\Phi_{NN}(r)=(2\pi b_N^2/3)^{-3/4}\exp(-3r^2/4b_N^2)$. Therefore, for any relative NN wave function Φ_{NN} we have the following constraints:

$$0\leqslant\langle P_{36}^X\rangle\leqslant 1 \quad \text{or} \quad 9\leqslant\mathcal{N}^2\leqslant 10. \tag{16}$$

The value (15) is equal to the usual identity factor $\sqrt{6!/3!3!2}$, well known in nuclear cluster physics (see, e.g., [24]). It plays an important role for the projection of six-quark configurations onto baryon-baryon channels [20]. From now on we shall omit the antisymmetrizer $\hat{\mathcal{A}}$ in front of the final state in the decay matrix element, but the identity factor (15) may not be omitted:

$$\begin{aligned}\langle d'|\hat{\mathcal{O}}_{\pi q}(\mathbf{k})|\Psi_{NN}(\mathbf{q}),\pi\rangle&=\langle d'|\hat{\mathcal{O}}_{\pi q}(\mathbf{k})\sqrt{10}\hat{\mathcal{A}}|\widetilde{\Psi}_{NN}(\mathbf{q}),\pi\rangle\\&=\sqrt{10}\langle d'|\hat{\mathcal{O}}_{\pi q}(\mathbf{k})|\widetilde{\Psi}_{NN}(\mathbf{q}),\pi\rangle.\end{aligned} \tag{17}$$

The inclusion of this factor, due to the antisymmetrization of the final two-nucleon wave function on the quark level, improves considerably the agreement of the results obtained in Ref. [8] with the experimentally suggested width.

D. Transition amplitude including intermediate states with up to two harmonic oscillator quanta

As in Ref. [8], we calculate the decay matrix element of Eq. (17) by inserting a complete set of six-quark configurations with quantum numbers of the final $^1S_0$ two-nucleon state ($LST=001$, $J^P=0^+$)

$$\begin{aligned}\langle\Psi_{NN}(\mathbf{q}),\pi|\hat{\mathcal{O}}_{\pi q}(\mathbf{k})|d'\rangle=\sqrt{10}\sum_{(n),\{f\}}&\langle\Phi_{NN}^{L=0}(\mathbf{q})\{N(123)N(456)\}_{ST=01}|(n,b_6),\{f\},LST=001\rangle\\&\times\langle(n,b_6),\{f\},LST=001|\hat{\mathcal{O}}_{\pi q}(\mathbf{k})|s^5p(b_6)[51]_X,[2^21^2]_{CT}LST=110,J^P=0^-\rangle.\end{aligned} \tag{18}$$

Here, $\{f\}=\{[f_X],[f_{CT}]\}$ and (n) defines quark states with n harmonic oscillator (HO) excitation quanta, i.e., $(n)=s^{6-n}p^n$, $s^{6-2m}(2s)^m$, $(n=2m)$, etc., and b_6 is the HO parameter for the six-quark system. The summation in Eq. (18) extends over a limited set of Young schemes $[f_X]$ and $[f_{CT}]$: The possible representations of $[f_{CT}]$ in the sum in Eq. (18) are given by the series of inner products of the $[2^3]_C$ color and $T=1[42]_T$ isospin Young schemes

$$\begin{aligned}[2^3]_C\circ[42]_T=&[42]_{CT}+[321]_{CT}+[2^3]_{CT}+[31^3]_{CT}\\&+[21^4]_{CT}.\end{aligned} \tag{19}$$

Only two spatial Young schemes $[6]_X$ and $[42]_X$ are compatible with the even-parity ($L=0$) N-N partial wave. Further constraints follow from the Pauli exclusion principle, i.e., $[f_X]\circ[33]_S\circ[f_{CT}]=[1^6]_{XCST}$. In the case of full spatial symmetry $[6]_X$, only one color-isospin state $[2^3]_{CT}$ is allowed, but the Young scheme $[42]_X$ of the excited shell-model configurations is compatible with each state from the inner product given in Eq. (19). Our choice of a one-body transition (pion-production) operator defined in Eq. (3) further restricts the number of relevant intermediate states. The one-particle operator (3) can excite (or deexcite) only one quark of the initial s^5p state. Therefore, the complete set of states in Eq. (18) is reduced to the configurations s^6, s^4p^2, and s^52s, knowing that higher one-particle excitations can be omitted because of a very small overlap with the final NN state. Summarizing, the following intermediate states are taken into account in Eq. (18): (i) the energetically lowest $(n=0)$ spatially symmetric state $s^6[6]_X[2^3]_{CT}$, (ii) the excited $(n=2)$ translationally invariant (orthogonalized to the $2S$ excitation of the six-quark c.m.) state $(s^4p^2-s^52s)$ with identical Young schemes $[6]_X$, $[2^3]_{CT}$, and (iii) five excited $(n=2)$ states $s^4p^2[42]_X[f_{CT}]$ with CT Young schemes from the inner product of Eq. (19).

It is interesting to note that all these configurations are also important for explaining the short-range nucleon-nucleon interaction. This was pointed out almost two decades ago [14,15,21] and thereafter discussed in many papers (see, e.g., [28] and references therein). Now we believe that a possible d' dibaryon has much potential for providing additional information on the innermost part of the nucleon-nucleon interaction, i.e., in the region where the nucleons overlap.

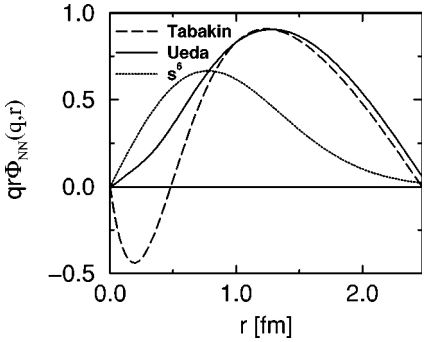

FIG. 2. Wave functions of the final $^1S_0$ state for two NN interaction models [22,23] at fixed laboratory energy $E_{NN}=100$ MeV. The projection of the s^6 six-quark configuration onto the NN channel is also shown.

E. Final state interaction

To take into account the FSI for the two outgoing nucleons, we consider separable-potential representations of the N-N interaction, namely, the phenomenological potential of Tabakin [22] and the separable model of Ueda *et al.* [23], which is equivalent to the one-boson exchange potential (OBEP). The wave functions of the $^1S_0$ NN final states for the Tabakin potential are of the form

$$\Phi_{NN}^{L=0}(q,r)=(2\pi)^{-3/2}\cos\delta_0\left\{ j_0(qr)-\tan\delta_0 n_0(qr) + A(q)\frac{e^{-\beta r}}{r}+B_1(q)\frac{e^{-\alpha r}}{r}\cos\alpha r + B_2(q)\frac{e^{-\alpha r}}{r}\sin\alpha r\right\}, \tag{20}$$

while the separable potential model of Ueda *et al.* leads to the $^1S_0$ NN wave function

$$\Phi_{NN}^{L=0}(q,r)=(2\pi)^{-3/2}\cos\delta_0\left\{ j_0(qr)-\tan\delta_0 n_0(qr) + \widetilde{A}(q)\,\frac{e^{-\gamma r}}{r}-\sum_{n=1}^{N}\widetilde{B}_n(q)\frac{e^{-\beta_n r}}{r}\right\}. \tag{21}$$

Here, $\delta_0(q)$ is the phase shift of NN scattering in the $^1S_0$ wave, and the functions A, $\widetilde{A}$, B_i, and $\widetilde{B}_i$ depend on the choice of parameters α, β, γ, and β_i for the two models (see the Appendix).

We use the nonstandard Tabakin potential because at short range the NN wave functions obtained with this potential differ qualitatively from OBEP wave functions. In Fig. 2, the wave functions (20) and (21) for both models are shown at an NN laboratory energy of $E_{NN}=100$ MeV. The relative wave function of Eq. (20) has a node at distances $r\approx 0.4$–0.5 fm (a stable position of the node in a large interval of NN energies produces the same NN-scattering phase shifts as a repulsive core). The two models are phase equivalent, but differ in their off-shell behavior. In the following we will demonstrate that the results for $\Gamma_{d'}$ differ considerably for both models, especially if the dibaryon mass $M_{d'}$ comes close to the πNN threshold.

III. EXPLICIT CALCULATION USING THE FRACTIONAL PARENTAGE COEFFICIENT (FPC) TECHNIQUE

Our approximation for the decay amplitude in Eq. (18) leads to a sum over products of two factors. The first factor is the so-called overlap integral of the intermediate six-quark configuration with the outgoing two-nucleon state. The second factor is a shell-model transition matrix element that describes the production of the pion on a single quark in the dibaryon and the subsequent transition to an intermediate six-quark configuration. Both factors can be calculated with the standard fractional parentage coefficient (FPC) technique, which was developed for quark-model calculations, for example, in Refs. [14–20].

A. Overlap integral of intermediate six-quark configurations with the NN continuum

In this subsection, we calculate the overlap integral of an intermediate six-quark configuration $(n,b_6)\{f\}$ with the (antisymmetrized and normalized) $^1S_0$ partial wave of the final NN state introduced in Eq. (9):

$$\langle\Psi_{NN}^{L=0}(q)|(n,b_6)\{f\}\rangle=\sqrt{10}\langle\Phi_{NN}^{L=0}(q)\{N((00,b_N)123) \times N((00,b_N)456)\}_{ST=01} \times|(n,b_6),[f_X],[f_{CT}],LST=001\rangle. \tag{22}$$

Beginning with Eq. (22) we denote from now on the nucleon wave function of Eq. (6) of the translationally invariant shell model as

$$N(123)\equiv N((n'l'=00,b_N)123). \tag{23}$$

Here l' is the total orbital angular momentum contained in the internal Jacobi coordinates $\boldsymbol{\rho}$, $\boldsymbol{\lambda}$, and b_N is the HO size parameter for the three-quark system.

The overlap integral (22) is calculated using the standard FPC technique for the quark shell model [15,17–20]. For this purpose we use a FPC decomposition of the six-quark configuration $(n,b_6)\{f\}$ into two three-quark clusters with CST quantum numbers of baryons $\{B_1((n'l',b_6)123)B_2((n''l'',b_6)456)\}_{CST}$. Note that for this procedure, the size parameter in the decomposition b_6 differs from the nucleonic size parameter b_N:

$$|(n,b_6)[f_X][f_{CT}]LST=001\rangle=\sum_{B_1(n')}\sum_{B_2(n'')}\sqrt{\frac{n_{f'_X}n_{f''_X}}{n_{f_X}}}\,U^{B_1B_2}_{\{f\}}\cdot C^{(n)}_{f_X}(n',n'')\{\ \varphi_{\tilde{N}\tilde{L}}(r,\sqrt{2/3}b_6)Y_{\tilde{L}\tilde{M}}(\hat{\mathbf{r}})$$
$$\times\{B_1((n'l',b_6)123)B_2((n''l'',b_6)456)\}_{ST=01}\}_{L=0}. \tag{24}$$

In expansion (24), $\varphi_{\tilde{N}\tilde{L}}(r,\mu r_0)$ is a HO wave function in the relative coordinate r of the two baryons with angular momentum $\vec{\tilde{L}}=\vec{L}-(\vec{l}'+\vec{l}'')$ and $\tilde{N}=n-(n'+n'')$ excitation quanta ($\mu r_0=\sqrt{2/3}b_6$ is the HO size parameter). As usual, n_{f_X} is the dimension of the IR $[f_X]$ of the permutation symmetry group S_6 for six particles [25]. $n_{f'_X}$ and $n_{f''_X}$ are the dimensions of IR's $[f'_X]$ and $[f''_X]$ of the subgroups S'_3 and S''_3 in the reduction $S_6\supset S'_3\times S''_3$. The coefficients $U^{B_1B_2}_{\{f\}}$ and $C^{(n)}_{f_X}(n',n'')$ are FPC's in the CST and X subspaces, respectively. For simplicity, we omit in Eq. (24) the indices for the dependence of $U^{B_1B_2}_{\{f\}}$ and $C^{(n)}_{f_X}(n',n'')$ on the intermediate Young schemes $f'_{CST}\equiv\tilde{f}'_X$, $f''_{CST}\equiv\tilde{f}''_X$, f'_{CT}, f''_{CT}, f'_S, f''_S, f'_T, f''_T, f'_C, and f''_C occurring for our chosen reduction chain of Eq. (2).

With the help Eq. (24), we can calculate the overlap (22). The three-quark-three-quark decomposition is, of course, the most adequate expansion for projecting onto the NN channel. The projection for a given intermediate state $(n)\{f\}$,

$$\Phi^{L=0}_{(n)\{f\}}(r)=\sqrt{10}\langle\{N((00,b_N)123)N((00,b_N)456)\}_{ST=01}$$
$$\times|(n,b_6)[f_X][f_{CT}]LST=001\rangle, \tag{25}$$

receives nonvanishing contributions only from NN components in Eq. (24) because non-nucleonic clusterings, such as $B_1(123)B_2(456)$, are orthogonal to $N(123)N(456)$ in CST space. Furthermore, the overlap of excited nucleonic clusters, e.g., $N((20,b_6)123)$, with the ground state nucleon $N((00,b_N)123)$ can be neglected if we assume that the size parameter b_6 of the six-quark configuration (24) does not differ considerably from the quark core radius b_N of the nucleon. In fact, because $b_6\neq b_N$, the nonzero overlap integral between excited and nonexcited nucleons is

$$\langle N((20,b_6)123)|N((00,b_N)123)\rangle$$
$$=\frac{(b_6^2/b_N^2-1)}{(1+b_6^2/b_N^2)}\left(\frac{2b_6/b_N}{1+b_6^2/b_N^2}\right)^3. \tag{26}$$

TABLE I. The CST part of the FPC three-quark–three-quark decomposition for the projection onto the NN channel $U^{NN}_{\{f\}}$, $\{f\}=\{[f_{CTS}],[f_{CT}]\}$.

$[f_{CTS}]$	$[1^6]_{CTS}$	$[2^21^2]_{CTS}$				
$[f_{CT}]$	$[2^3]_{CT}$	$[42]_{CT}$	$[321]_{CT}$	$[2^3]_{CT}$	$[31^3]_{CT}$	$[21^4]_{CT}$
$U^{NN}_{\{f\}}$	$\sqrt{\frac{1}{9}}$	$-\sqrt{\frac{9}{20}}$	$\sqrt{\frac{16}{45}}$	$\sqrt{\frac{1}{36}}$	$-\sqrt{\frac{1}{18}}$	0

The sum over all possible terms gives a negligible contribution to the final result because the different terms interfere destructively (see next section). Because of these restrictions, we are led to the expression

$$\Phi^{L=0}_{(n)\{f\}}(r)\approx\langle N((00,b_N)123)|N((00,b_6)123)\rangle$$
$$\times\langle N((00,b_N)456)|N((00,b_6)456)\rangle\sqrt{10}$$
$$\times\sqrt{\frac{1}{n_{f_X}}}\,U^{NN}_{\{f\}}C^{(n)}_{f_X}(0,0)\varphi_{n0}(r,\sqrt{2/3}b_6)Y_{00}(\hat{r}), \tag{27}$$

where

$$C^{(n)}_{f_X}(0,0)=\begin{cases}1, & \text{if } n=0, \quad [f_X]=[6],\\ -\sqrt{\frac{1}{5}}, & n=2, \quad [f_X]=[6],\\ -\sqrt{\frac{4}{5}}, & n=2, \quad [f_X]=[42].\end{cases}$$

The coefficients $C^{(n)}_{f_X}(n',n'')$ are calculated by general methods from the TISM (see, e.g., Ref. [24]). The values of $U^{NN}_{\{f\}}$ are given in Table I. The general rule for calculating FPC's in the CST subspace is the factorization of the value $U^{B_1B_2}_{\{f\}}$ [14–18] (symbolically),

$$U^{B_1B_2}_{\{f\}}=\mathrm{SF}_{CT\cdot S}\mathrm{SF}_{C\cdot T}, \tag{28}$$

in terms of scalar factors $\mathrm{SF}_{CT\cdot S}$ and $\mathrm{SF}_{C\cdot T}$ of Clebsch-Gordan coefficients of the unitary groups $\mathrm{SU}(12)_{CST}$ and $\mathrm{SU}(6)_{CT}$ for the reductions $\mathrm{SU}(12)_{CST}\supset\mathrm{SU}(6)_{CT}\times\mathrm{SU}(2)_S$ and $\mathrm{SU}(6)_{CT}\supset\mathrm{SU}(3)_C\times\mathrm{SU}(2)_T$, respectively [which are links of the common reduction chain (2)]. The necessary SF's are tabulated in Refs. [15–20]. With expression (27), the overlap integral of Eq. (22) reduces to

$$\langle\Psi^{L=0}_{NN}(q)|(n,b_6)\{f\}\rangle=\langle\Phi^{L=0}_{NN}(q)|\Phi^{L=0}_{(n)\{f\}}\rangle$$
$$\approx\sqrt{10}\left(\frac{2b_6/b_N}{1+b_6^2/b_N^2}\right)^6\sqrt{\frac{1}{n_{f_X}}}\,U^{NN}_{\{f\}}C^{(n)}_{f_X}$$
$$\times(0,0)\left(\frac{8\pi b_6^2}{3}\right)^{3/4}I^{(n)}_{NN}(q). \tag{29}$$

Equation (29) contains a simple radial integral

$$\left(\frac{8\pi b_6^2}{3}\right)^{3/4} I_{NN}^{(n)}(q) = \sqrt{4\pi}\int_0^\infty r^2\, dr\ \Phi_{NN}^{L=0}(q,r)\varphi_{n0}(r,\sqrt{2/3}b_6), \tag{30}$$

which can be calculated analytically for a plane wave $\Phi_{NN}^{L=0}(q,r)=(2\pi)^{-3/2}j_0(qr)$, as well as for the Tabakin FSI wave functions of Eq. (20) and for the Ueda FSI wave functions given in Eq. (21). Results for $I_{NN}^{(n)}(q)$ are listed in the Appendix. The large brackets in Eq. (29) involving the ratio of the two HO size parameters b_N/b_6 come from the overlap of the two nucleon clusters

$$\langle N((00,b_N)123)|N((00,b_6)123)\rangle \times\langle N((00,b_N)456)|N((00,b_6)456)\rangle.$$

B. Shell-model transition matrix element

The shell-model matrix element of the pion-production operator $\hat{\mathcal{O}}_{\pi q}$ defined in Eq. (3) [the second factor in the decay amplitude introduced in Eq. (18)] is proportional to the one-particle matrix element of the spin-isospin-flip operator $\sigma_j^{(\mu)}\tau_j^{(\kappa)}$. The remaining five quarks act as spectators for the transition. Chosing the sixth quark, we write the matrix element for the emission of a π^-:

$$\begin{aligned}\langle (n,b_6)\{\overline{f}\}\overline{LST}=001,J^P=0^+,T_z=1;\pi^-|\hat{\mathcal{O}}_{\pi q}(\mathbf{k})|d'\rangle &= 6\,\frac{f_{\pi q}}{m_\pi}\,\frac{k}{\sqrt{2E_\pi(2\pi)^3}}\langle (n,b_6)\{\overline{f}\}\overline{LST}\\ &=001,T_z=1|(\boldsymbol{\sigma}_6\cdot\hat{\mathbf{k}})\tau_6^{(+)}\\ &\times\exp\left(i\frac{5}{6}\mathbf{k}\cdot\boldsymbol{\rho}_6\right)|d'\rangle.\end{aligned} \tag{31}$$

Here, $\boldsymbol{\rho}_6=\mathbf{r}_6-\frac{1}{5}\Sigma_{i=1}^5\mathbf{r}_i$, is the Jacobi coordinate, and $\boldsymbol{\sigma}_6$ and $\boldsymbol{\tau}_6$ are spin and isospin of the sixth quark. The momentum of the pion is $\mathbf{k}=k\hat{\mathbf{k}}$, and the factor of 6 in front of the one-particle matrix element contains the summation over all six quarks. The natural choice for a FPC decomposition is clearly the separation of the last quark $q^6\to q^5\times q$ (one-particle FPC), which allows one to exploit the orthogonality constraints for the five spectator quarks. With the one-particle FPC expansion of the shell-model states, the right-hand side of Eq. (31) reduces to a sum of one-particle spin-isospin-flip amplitudes with algebraic coefficients:

$$\begin{aligned}\langle (n,b_6)\{\overline{f}\}\overline{LST}=001,T_z=1|(\boldsymbol{\sigma}_6\cdot\hat{\mathbf{k}})\tau_6^{(+)}e^{-i\,5\mathbf{k}\cdot\boldsymbol{\rho}_6/6}|d'\rangle &= \sum_{\overline{f}'_X}\sqrt{\frac{n_{\overline{f}'_X}}{n_{\overline{f}_X}}}\sum_{f'_X}\sqrt{\frac{n_{f'_X}}{n_{f_X}}}\sum_{S',T'}U_{\{\overline{f}\}}(\overline{S'T'},S_6=T_6=1/2)\sum_{S',T'}U_{\{f\}}(S'T',S_6=T_6=1/2)\sum_M(1,-M,1,M|0,0)\\ &\times\{\delta_{n,2}C_{[51]_X}^{(1)}(s^4p,s)C_{f_X}^{(2)}(s^4p,p)X_6(\mathbf{k};11M,00)+C_{[51]_X}^{(1)}(s^5,p)[\,\delta_{n,0}C_{[6]_X}^{(0)}(s^5,s)\\ &+\delta_{n,2}C_{[6]_X}^{(2)}(s^5,2s)]X_6(\mathbf{k};11M,n0)\}\\ &\times 3i\langle\overline{S'},S_6:\overline{S}=0|(\boldsymbol{\sigma}_6\cdot\hat{\mathbf{k}})|S',S_6:S=1,M\rangle\langle\overline{T'},T_6:\overline{T}=T_z=1|\tau_6^{(+)}|T',T_6:T=0\rangle,\end{aligned} \tag{32}$$

where the functions $X_6(\mathbf{k};11M,n0)$ are spatial integrals:

$$X_6(\mathbf{k};11M,n0)=\int_{4\pi}(\hat{\mathbf{k}}\cdot\hat{\boldsymbol{\rho}}_6)Y_{1-M}(\hat{\boldsymbol{\rho}}_6)d^2\hat{\boldsymbol{\rho}}_6\int_0^\infty\rho_6^2 d\rho_6\varphi_{n0}(\rho_6,\sqrt{6/5}b_6)\varphi_{11}(\rho_6,\sqrt{6/5}b_6)j_1(5/6k\rho_6). \tag{33}$$

Here S' and T' ($\overline{S'}$ and $\overline{T'}$) are the spin and isospin of the five spectator quarks after the separation of the sixth quark. The first term in the curly brackets on the right-hand side of Eq. (32) corresponds to the quark transition from an initial s state to a final p state. The second term corresponds to the quark transition from an initial p state to a final s or $2s$ state. In Eq. (32), we use almost the same notation for the one-particle FPC's $U_{\{f\}}(S'T',S_6T_6)$ and $C_{f_X}^{(n)}((n'),(n''))$ as before for the three-particle FPC's in Eq. (24). Note that the one-particle FPC $U_{\{f\}}(S'T',S_6T_6)$ in the CST subspace can be calculated with one-particle scalar factors SF [cf. Eq. (28)], which can be found for example in Ref. [19].

Because of the orthogonality restrictions for the five spectator quarks, the summations over $\overline{f'_X}$, f'_X, S', T', S', and

T' collapse to $\delta_{\overline{f'_X},f'_X}$, $\delta_{\overline{S'},S'}$, $\delta_{\overline{S'},S_6}$, $\delta_{\overline{T'},T'}$, and $\delta_{\overline{T'},T_6}$, and the only nonvanishing elementary spin- and isospin-flip amplitudes in Eq. (32) are

$$\langle \overline{S'}=S_6=1/2:\overline{S}=0|\sigma_6^{(\mu)}|S'=S_6=1/2:S=1,-M\rangle = -(-1)^{\mu}\delta_{\mu M},$$

$$\langle \overline{T'}=T_6=1/2:\overline{T}=1,\overline{T_z}|\tau_6^{(\kappa)}|T'=T_6=1/2:T=0\rangle = (-1)^{\kappa}\delta_{\kappa\overline{T_z}}. \quad (34)$$

C. Decay amplitude after summation over allowed intermediate states

Collecting the shell-model matrix element of Eqs. (31) and (32) for pion production and the overlap integrals of Eq. (29) for all intermediate six-quark configurations, and performing the remaining radial integrals in Eqs. (30) and (33), leads to the following result for the full decay amplitude defined in Eq. (18):

$$\langle \Psi_{NN}(\mathbf{q}),\pi^-|\hat{\mathcal{O}}_{\pi q}(\mathbf{k})|d'\rangle = -\frac{10i}{27(2\pi)^{3/2}}\left(\frac{2}{3\pi}\right)^{3/4}\frac{f_{\pi q}}{m_\pi}\sqrt{\frac{b_6}{E_\pi}}\left(\frac{2b_6/b_N}{1+b_6^2/b_N^2}\right)^6(kb_6)^2 \times \exp\left(-\frac{5}{24}k^2b_6^2\right)\left[I_{NN}^{(0)}(q)+\sqrt{\frac{2}{27}}\left(1-\frac{k^2b_6^2}{24}\right)I_{NN}^{(2)}(q)\right]. \quad (35)$$

The overlap integrals $I_{NN}^{(0)}(q)$ and $I_{NN}^{(2)}(q)$ can be found in the Appendix. Note that the inclusion of overlap terms with excited nucleon configurations in the intermediate six-quark states, originating from the different harmonic oscillator parameters $b_6 \neq b_N$, given in Eq. (26), leads to a nonessential renormalization factor of the decay amplitude (35),

$$1-\frac{1}{5\sqrt{6}}\frac{(b_6^2/b_N^2-1)}{(1+b_6^2/b_N^2)}\left(1-\frac{5}{6}k^2b_6^2\right), \quad (36)$$

in front of the term $I_{NN}^{(0)}(q)$ on the right-hand side of Eq. (35). This factor (36) can be omitted for small kb_6. The k^2 behavior of the decay amplitude is due to (i) a factor k in the transition operator of Eq. (3) and (ii) due to the fact that a p-wave quark is involved either in the initial or the final state of the one-particle transition matrix element on the right-hand side of Eq. (32). We recall that in the case of the Δ-isobar decay into the πN channel, the transition matrix element is proportional only to k^1, corresponding to the $\boldsymbol{\sigma}_j\cdot\mathbf{k}$ term in Eq. (3). The k^2 behavior of the d' decay amplitude (35) leads to a very strong dependence of the d' decay width on the value of $M_{d'}$, as we will see in the next section.

IV. NUMERICAL RESULTS AND DISCUSSION

The total hadronic decay width of the possible d' dibaryon $\Gamma_{d'}$ contains three partial widths

$$\Gamma_{d'}=\Gamma_{\pi^-pp}+\Gamma_{\pi^0pn}+\Gamma_{\pi^+nn}=3\Gamma_{\pi^-pp}, \quad (37)$$

which are equal to each other $\Gamma_{\pi^-pp}=\Gamma_{\pi^0pn}=\Gamma_{\pi^+nn}$, when we neglect isospin-breaking effects. The partial π^-pp decay width Γ_{π^-pp} is defined by the standard expression [8]

$$\Gamma_{\pi^-pp}=2\pi\int d^3q\int d^3k\,\delta\left(M_{d'}-2M_N-\frac{k^2}{4M_N}-\frac{q^2}{M_N}-\sqrt{m_\pi^2+k^2}\right)|\langle\Psi_{NN}(\mathbf{q}),\pi^-|\hat{\mathcal{O}}_{\pi q}(\mathbf{k})|d'\rangle|^2, \quad (38)$$

where $\mathbf{q}=(\mathbf{q}_1-\mathbf{q}_2)/2$ is the relative momentum of the two final protons and $\mathbf{k}$ is the momentum of emitted pion in the c.m. of the d' dibaryon. The δ function conserves the energy in the decay, while integration over the momentum-conserving $\delta^{(3)}(\mathbf{q}_1+\mathbf{q}_2+\mathbf{k})$ has already been exploited [8] in Eq. (38). The integration over three-particle phase space leads to the following result for the partial $d'\to\pi^-pp$ decay width:

$$\Gamma_{\pi^-pp}=\frac{2^5 10^2\sqrt{6}}{3^8\sqrt{\pi}}\frac{f_{\pi q}^2}{4\pi}\frac{1}{m_\pi^2}\left(\frac{2b_6/b_N}{1+b_6^2/b_N^2}\right)^{12} \times\int_0^{q_{\max}}\frac{2M_N(k_0b_6)^5}{2M_N+\sqrt{m_\pi^2+k_0^2}}\exp\left(-\frac{5}{12}k_0^2b_6^2\right) \times\left[I_{NN}^{(0)}(q)+\sqrt{\frac{2}{27}}\left(1-\frac{k_0^2b_6^2}{24}\right)I_{NN}^{(2)}(q)\right]^2 q^2\,dq. \quad (39)$$

Here, energy conservation relates the pion momentum k_0 to the NN relative momentum q via

$$k_0(q)=\left\{4M_N\left[\left(M_{d'}-\frac{q^2}{M_N}\right)-\sqrt{\left(M_{d'}-\frac{q^2}{M_N}\right)^2-\left(M_{d'}-2M_N-\frac{q^2}{M_N}\right)^2+m_\pi^2}\right]\right\}^{1/2},$$

TABLE II. Calculated π^- decay width $\Gamma_{\pi^- pp}$ and the total hadronic decay width $\Gamma_{d'}$ of the d' dibaryon for five different d' masses and wave functions (b_6 is the characteristic d' size parameter, and b_N is the quark core radius of the nucleon). Masses and wave functions of the d' were obtained in Refs. [6,7] within different models for the microscopic q-q interaction.

				$\Gamma_{\pi^- pp}$ [MeV]			$\Gamma_{d'}$ [MeV]		
Set	b_N [fm]	b_6 [fm]	$M_{d'}$ [MeV]	PW	T	U	PW	T	U
1	0.45	0.59	2705	56.8(44.1)	7.8(5.2)	41.2(46.0)	170.5	23.3	123.6
2	0.47	0.65	2680	44.2(35.7)	8.3(7.0)	32.6(36.5)	132.5	24.9	97.8
3	0.6	1.24	2162	0.22(0.17)	0.27(0.18)	0.25(0.22)	0.67	0.81	0.76
4	0.595	0.78	2484	28.3(22.6)	10.9(8.9)	21.8(21.9)	84.8	32.6	65.4
5	0.595	0.95	2092	0.058(0.036)	0.061(0.049)	0.107(0.071)	0.173	0.183	0.321

and for $q_{\max}=\sqrt{M_N(M_{d'}-2M_N-m_\pi)}$ all available decay energy is converted to kinetic energy in the relative NN system, and none to the pion $E_\pi=m_\pi$, $k_0=0$.

The calculated decay widths are shown in Table II, where we have introduced the abbreviations PW, T, and U. Here, PW refers to a calculation employing a plane-wave final N-N state (4), while T and U refer to calculations using the Tabakin [22] (T) and Ueda *et al.* [23] (U) separable NN potentials for the final state interaction.

In parentheses we give the results obtained in the approximation of using only one intermediate six-quark configuration s^6 $(n=0)$. With the exception of the results for the Ueda NN potential for sets 1, 2, and 4 (for which the d' mass is 400–650 MeV above the πNN threshold), the inclusion of all Pauli-principle-allowed intermediate $2\hbar\omega$ shell-model configurations tends to increase the decay width by some 20–30%. The largest effect is obtained for d' masses rather close to threshold, exemplarily shown for sets 3 and 5.

It can be seen from Table II and Fig. 3 that the pionic decay width of the d' is very sensitive to the dibaryon mass $M_{d'}$, which determines the available phase space of the three-body πNN decay. The sensitivity grows dramatically near the πNN threshold (2016 MeV). If we extrapolate the results of Table II to the experimental value of $M_{d'}$ $=2065$ MeV, we obtain a very strong reduction of $\Gamma_{d'}$ as compared with the quite realistic variants (sets 3 and 5) in Table II:

$$\Gamma_{d'}^{\rm PW}=0.032\ \text{MeV},\quad \Gamma_{d'}^{\rm T}=0.046\ \text{MeV},\quad \Gamma_{d'}^{\rm U}=0.083\ \text{MeV},$$
$$\text{if } b_N=0.595\ \text{fm} \quad \text{and } b_6=0.95\ \text{fm};$$

$$\Gamma_{d'}^{\rm PW}=0.018\ \text{MeV},\quad \Gamma_{d'}^{\rm T}=0.045\ \text{MeV},\quad \Gamma_{d'}^{\rm U}=0.040\ \text{MeV},$$
$$\text{if } b_N=0.6\ \text{fm} \quad \text{and } b_6=1.24\ \text{fm}.$$

This strong dependence of $\Gamma_{d'}$ on the value of $M_{d'}$ is a consequence of the high power of $(k_0 b_6)^5$ in the integrand of Eq. (39). The origin of this k_0^5 behavior (compared with a k_0^3 behavior in case of the Δ-isobar decay) comes, as explained above, from the necessity to excite (or deexcite) a p-wave quark for the production of a pion. Note that for small $q_{\max}$ (when $M_{d'}$ is close to the πNN threshold) the function $k_0(q)$ is linear in the factor $\sqrt{q_{\max}^2-q^2}$ and can be written as $k_0(q)\approx q_{\max}\sqrt{4m_\pi(1-q^2/q_{\max}^2)/M_{d'}}$. Therefore, for small $q_{\max}$ the integral in Eq. (39) behaves as $q_{\max}^8$. The second high-power factor in Eq. (39) is the scale factor

$$\left(\frac{2b_6/b_N}{1+b_6^2/b_N^2}\right)^{12},$$

which depends sensitively on the ratio b_6/b_N. However, this sensitivity is considerably reduced by the factor b_6^5 in the integrand. The product

$$b_6^5\left(\frac{2b_6/b_N}{1+b_6^2/b_N^2}\right)^{12}$$

is a quite smooth function of b_N/b_6. For $b_N=0.6$ fm this product varies from 0.078 fm^5 to 0.158 fm^5, if b_6 varies from 0.6 fm to 1.24 fm.

For small $q_{\max}$, FSI's make an important contribution to the d' decay width because of the large scattering length in the $^1S_0$ wave $a_s=-23.7$ fm. The FSI enhances the decay width for example by about 85% for set 5 in Table II. At the experimental mass $M_{d'}=2065$ MeV, the hadronic decay width is more than doubled by the final state interaction. It is interesting that in the case of the Tabakin model with a nodal

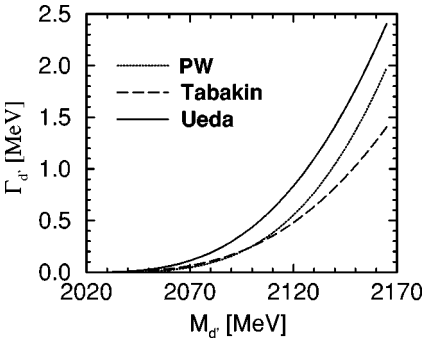

FIG. 3. Pionic decay width $\Gamma_{d'}$ of the d' as a function of the dibaryon mass $M_{d'}$ for different final state interactions (FSI's) between the outgoing nucleons: (i) plane wave (PW, dotted curve), (ii) with FSI's using the Tabakin [22] potential (dashed curve), and (iii) with FSI's using the Ueda *et al.* [23] potential (plain curve). The harmonic oscillator parameters $b_N=0.595$ fm and $b_6=0.95$ fm are those of set 5 in Table II. The πNN threshold for the decay is at 2016 MeV, while the experimentally suggested resonance position of the d' is at 2065 MeV.

TABLE III. Radial integrals $I^{(n)}_{NN}(q)$ for plane waves (PW) and FSI functions given in Eqs. (20) and (21) for the Tabakin [22] and Ueda [23] separable potential formulation of the relative NN wave function.

Model	$I^{(0)}_{NN}(q)=$	$I^{(2)}_{NN}(q)=$
PW	$f^{(0)}(qb_6)$	$f^{(2)}(qb_6)$
Tabakin Eq. (20)	$\cos\delta_0[f^{(0)}(qb_6)+\tan\delta_0 g^{(0)}(qb_6)$ $+A(q)\alpha F^{(0)}(\alpha b_6)+B_1(q)\beta G^{(0)}_1(\beta b_6)$ $+B_2(q)\beta G^{(0)}_2(\beta b_6)]$	$\cos\delta_0[f^{(2)}(qb_6)+\tan\delta_0 g^{(2)}(qb_6)$ $+A(q)\alpha F^{(2)}(\alpha b_6)+B_1(q)\beta G^{(2)}_1(\beta b_6)$ $+B_2(q)\beta G^{(2)}_2(\beta b_6)]$
Ueda Eq. (21)	$\cos\delta_0[f^{(0)}(qb_6)+\tan\delta_0 g^{(0)}(qb_6)$ $+\widetilde{A}(q)\gamma F^{(0)}(\gamma b_6)-\Sigma_n\widetilde{B}_n(q)\beta_n F^{(0)}(\beta_n b_6)]$	$\cos\delta_0[f^{(2)}(qb_6)+\tan\delta_0 g^{(2)}(qb_6)$ $+\widetilde{A}(q)\gamma F^{(2)}(\gamma b_6)-\Sigma_n\widetilde{B}_n(q)\beta_n F^{(2)}(\beta_n b_6)]$

NN wave function at short range, the contribution from FSI's is smaller than for the Ueda model and can even decrease the width compared to the plane wave result (cf. set 4). This is a direct consequence of an approximate orthogonality of the nodal wave function of the Tabakin model to the projection of the intermediate s^6 configuration (i.e., the HO function φ_{00}) of Eq. (27) onto the NN channel. This can easily be seen from Fig. 2, where both wave functions are shown. The approximate orthogonality of the functions φ_{00} and $\Phi^{\rm Tabakin}_{NN}$ in the integrand of Eq. (29) reduces considerably the overlap factor $I^0_{NN}(q)$, which gives the dominant contribution to the d' decay width (see values in parentheses in Table II). As can be seen in Fig. 3, the disagreement between the Tabakin and Ueda models grows with increasing dibaryon mass $M_{d'}$ (the influence of the large scattering length a_s, which is common for both models, becomes negligible compared to the effect of the larger phase space). For sets 1, 2, and 4 in Table II, the Tabakin model leads again to values of $\Gamma_{d'}$, which are even smaller than $\Gamma_{d'}$ in the plane wave approximation neglecting FSI's.

V. SUMMARY

In this work we have studied the pionic decay of a possible d' dibaryon within the microscopic quark shell model. We use a single-quark transition operator which describes the production of the pion on a single quark. The dibaryon wave function is given as a single six-quark translationally invariant shell-model configuration, which has been found to provide an adequate description of the d' [6,7]. Previous results from [8] have been improved mainly in three points, leading to a complete calculation in the sense that (i) the calculation is performed consistently on the quark level, i.e., the final two-nucleon state is normalized and antisymmetrized on the quark level, (ii) all important intermediate six-quark states with nonvanishing overlaps with the final two nucleons are included, and (iii) the strong final state interaction for the two nucleons is taken into account on the basis of the separable Tabakin [22] and Ueda [23] NN potentials.

Not surprisingly, the small available phase space in the three-body decay is the dominant mechanism for the narrow width of the d'. The large identity factor (15), on the other hand, enhances the results of previous evaluations disregarding the identity of quarks from different nucleons. The inclusion of all Pauli-principle-allowed intermediate $2\hbar\omega$ shell-model configurations tends to increase the decay width by some 20–30%. Furthermore, the final state interaction for the two outgoing nucleons also increases the decay width considerably, if the d' mass is close to the πNN threshold. Because of these three effects, the calculated pionic decay widths lie between $\Gamma_{d'}=0.18-0.32$ MeV for the most realistic set 5, having a d' mass close to the experimentally suggested one and a characteristic hadronic size of the dibaryon of $b_6\approx 1$ fm. This qualitatively agrees with the experimentally suggested value $\Gamma_{d'}=0.5$ MeV.

Despite the fact that both the Tabakin and Ueda FSI models, are unsuitable for large NN energies (as in parameter sets 1, 2, and 4), the two models demonstrate the strong influence of the short-range behavior of the NN wave function on the d' decay width (see, e.g., Figs. 2 and 3). Recall that these two models are typical representatives of qualitatively different classes of NN phenomenology. Whereas the Ueda separable potential is an approximation of the OBEP, i.e., a model with short-range repulsion, the Tabakin potential can be considered as a unitary-pole approximation (UPA) [26] of a Moscow-type potential model [27] with short-range attraction and forbidden states. The Moscow model proceeds from the assumption of a six-quark origin of the short-range NN interaction and pretends to give an adequate description of the nonlocal character of the NN force. The main conclusion to be drawn here is that these two models, which are phase equivalent, differ considerably in their effect on the d' decay width. Therefore, a possible d' dibaryon would provide a natural laboratory for detailed studies of the short-range NN interaction.

An interesting continuation of this work would be to go beyond phenomenological NN potential models and use a completely microscopic quark model approach (see, e.g., [28] and references therein). For example, one could calculate the pionic decay of the d' dibaryon using a final $^1S_0$ NN-scattering wave function that is based on the same microscopic quark Hamiltonian which simultaneously describes the mass $M_{d'}$ and structure of the d' dibaryon. However, such a calculation is complicated by the fact that we have used two different Hamiltonians, i.e., two different confinement strengths, for three-quark baryons and the six-quark d' dibaryon [7]. Thus, the d' dibaryon could not be explained in terms of the standard constituent quark model, using a common Hamiltonian for any number of quarks. On the other hand, if the d' exists, this may be taken as an indication that the effective (nonperturbative) quark-quark interaction depends on the state of the system.

ACKNOWLEDGMENTS

Two of the authors (K.I. and I.T.O.) acknowledge the warm hospitality extended to them at the Institute for Theoretical Physics, University of Tübingen, where this work has been mostly completed. One of the authors (K.I.) wishes to thank the Ministry of Education, Science, Sports and Culture (Japan) for financial support. Partially, this work was supported by RFBR Grant No. 96-02-1807 and DFG Grant No. Fa-67/20-1, and one of the authors (I.T.O.) thanks RFBR for financial support. G.W. thanks the Deutsche Forschungsgemeinschaft (DFG) for support under Contract No. WA1147/1-1.

APPENDIX

In this appendix we present the analytical expressions for the radial integrals $I_{NN}^{(n)}(q)$ defined in Eq. (30), which are needed to calculate the overlap integral of Eq. (22) between different intermediate six-quark shell-model configurations and the two outgoing nucleons. We recall, that the relative NN wave function may be described by a simple plane wave (PW) $\Phi_{NN}^{L=0}(q,r)=(2\pi)^{-3/2}j_0(qr)$ or by FSI wave functions resulting, for example, from separable potential representations of the NN interaction. We use the results for the NN wave function obtained by Tabakin [22] given in Eq. (20) and the result obtained by Ueda and co-workers [23], given in Eq. (21). Note that coefficients $\widetilde{A}$ and $\widetilde{B}_n$ in Eq. (21) depend on parameters of the one-term separable potential of Ueda *et al.* [23], $V(q,q')=-M_{11}g(q)g(q')$, $g(q)=\Sigma_n c_n(q_c^2-q^2)/(q^2+\beta_n^2)(q^2+\gamma^2)$. For $\widetilde{A}$ and $\widetilde{B}_n$ we use the following expressions:

$$\widetilde{A}(q)=\alpha^2\frac{g(q)}{1-G(q)}\sum_n \frac{c_n}{\gamma^2-\beta_n^2}\left(\frac{\gamma^2+q_c^2}{\gamma^2+q^2}\right),$$

$$\widetilde{B}_n(q)=\alpha^2\frac{g(q)}{1-G(q)}\left(\frac{c_n}{\gamma^2-\beta_n^2}\right)\left(\frac{\beta_n^2+q_c^2}{\beta_n^2+q^2}\right),$$

where $\alpha^2=2\pi^2 m_N M_{11}/\hbar^2$, $G(q)=(2/\pi)\alpha^2\int_0^\infty[(g^2(k)k^2-g^2(q)q^2)/(k^2-q^2)]dk$, and a value of γ, which is not fixed in Ref. [23], is fitted to the singlet scattering length ($a_s=-23.7$ fm), $\gamma=11.114$ fm^{-1}.

In Table III we introduced the following abbreviations:

$$f^{(0)}(x)=e^{-x^2/3},$$

$$f^{(2)}(x)=-\sqrt{\frac{3}{2}}\left(1-\frac{4}{9}x^2\right)e^{-x^2/3},$$

$$g^{(0)}(x)=\frac{\sqrt{3}}{x\sqrt{\pi}}-e^{-x^2/3}\mathrm{Im}\Phi\left(\frac{ix}{\sqrt{3}}\right),$$

$$g^{(2)}(x)=-\sqrt{\frac{3}{2}}\left[\frac{\sqrt{3}}{x\sqrt{\pi}}\left(\frac{1}{3}-\frac{4}{9}x^2\right)-\left(1-\frac{4}{9}x^2\right)e^{-x^2/3}\ \mathrm{Im}\ \Phi\left(\frac{ix}{\sqrt{3}}\right)\right],$$

$$F^{(0)}(x)=\frac{\sqrt{3}}{x\sqrt{\pi}}-e^{x^2/3}[1-\Phi(x/3)],$$

$$F^{(2)}(x)=-\sqrt{\frac{3}{2}}\left\{\frac{\sqrt{3}}{x\sqrt{\pi}}\left(\frac{1}{3}+\frac{4}{9}x^2\right)-\left(1+\frac{4}{9}x^2\right)e^{x^2/3}[1-\Phi(x/3)]\right\},$$

$$G_1^{(0)}=\frac{\sqrt{3}}{x\sqrt{\pi}}+(\sin x^2/3-\cos x^2/3)[1-\mathrm{Re}\Phi((1+i)x/\sqrt{3})]-(\sin x^2/3+\cos x^2/3)\mathrm{Im}\Phi((1+i)x/\sqrt{3}),$$

$$G_2^{(0)}=(\sin x^2/3+\cos x^2/3)[1-\mathrm{Re}\Phi((1+i)x/\sqrt{3})]+(\sin x^2/3-\cos x^2/3)\mathrm{Im}\Phi((1+i)x/\sqrt{3}),$$

$$G_1^{(2)}=-\sqrt{\frac{3}{2}}\left\{\frac{\sqrt{3}}{x\sqrt{\pi}}+\left[\left(\frac{1}{3}+\frac{4}{9}x^2\right)\sin x^2/3-\left(\frac{1}{3}-\frac{4}{9}x^2\right)\cos x^2/3\right][1-\mathrm{Re}\Phi((1+i)x/\sqrt{3})]\right.$$
$$\left.-\left[\left(\frac{1}{3}-\frac{4}{9}x^2\right)\sin x^2/3+\left(\frac{1}{3}+\frac{4}{9}x^2\right)\cos x^2/3\right]\mathrm{Im}\Phi((1+i)x/\sqrt{3})\right\},$$

$$G_2^{(2)} = -\sqrt{\frac{3}{2}}\left\{-\frac{4}{9}x^2\frac{\sqrt{3}}{x\sqrt{\pi}} + \left[\left(\frac{1}{3}-\frac{4}{9}x^2\right)\sin x^2/3 + \left(\frac{1}{3}-\frac{4}{9}x^2\right)\cos x^2/3\right]\left[1-\mathrm{Re}\Phi((1+i)x/\sqrt{3})\right]\right.$$
$$\left.-\left[\left(\frac{1}{3}+\frac{4}{9}x^2\right)\sin x^2/3 - \left(\frac{1}{3}-\frac{4}{9}x^2\right)\cos x^2/3\right]\mathrm{Im}\Phi((1+i)x/\sqrt{3})\right\}.$$

[1] R. Bilger, B. M. Barnet, H. Clement, S. Krell, G. J. Wagner, J. Jaki, C. Joram, T. Kirchner, W. Kluge, M. Metzler, R. Wieser, and D. Renker, Phys. Lett. B **269**, 247 (1991); R. Bilger, H. Clement, K. Föhl, K. Heitlinger, C. Joram, W. Kluge, M. Schepkin, G. J. Wagner, R. Wieser, R. Abela, F. Foroughi, and D. Renker, Z. Phys. A **343**, 941 (1992); K. Föhl, Ph.D. thesis, University of Tuebingen, 1996; H. Clement, M. Schepkin, G. J. Wagner, and O. Zaboronsky, Phys. Lett. B **337**, 43 (1994).

[2] W. A. Kaminski, Phys. Part. Nucl. **26**, 148 (1995).

[3] H. Clement (private communication).

[4] B. V. Martemyanov and M. G. Schepkin, JETP Lett. **53**, 776 (1991); R. Bilger, H. A. Clement, and M. G. Schepkin, Phys. Rev. Lett. **71**, 42 (1993); R. Bilger, πN Newslett. **10**, 47 (1995).

[5] P. J. Mulders, A. T. Aerts, and J. J. de Swart, Phys. Rev. Lett. **40**, 1543 (1978); Phys. Rev. D **21**, 2653 (1980).

[6] Georg Wagner, L. Ya. Glozman, A. J. Buchmann, and Amand Faessler, Nucl. Phys. **A594**, 263 (1995); L. Ya. Glozman, A. J. Buchmann, and Amand Faessler, J. Phys. G **20**, L49 (1994).

[7] A. J. Buchmann, Georg Wagner, and Amand Faessler, Phys. Rev. C (submitted); A. J. Buchmann, Georg Wagner, K. Tsushima, Amand Faessler, and L. Ya. Glozman, πN Newslett. **10**, 68 (1995); Prog. Part. Nucl. Phys. **36**, 383 (1996).

[8] K. Itonaga, A. J. Buchmann, Georg Wagner, and Amand Faessler, Nucl. Phys. **A609**, 422 (1996).

[9] K. K. Seth, in *Pions in Nuclei*, edited by E. Oset (World Scientific, Singapore, 1992), p. 205.

[10] F. Wang, J.-L. Ping, G.-H. Wu, L.-J. Teng, and T. Goldman, Phys. Rev. C **51**, 3411 (1995).

[11] B. Schwesinger and N. N. Scoccola, Phys. Lett. B **363**, 29 (1995); H. Garcilazo and L. Mathelisch, Phys. Rev. Lett. **72**, 2971 (1994); A. Valcarce, H. Garcilazo, F. Fernandez, and E. Moro, Phys. Rev. C **54**, 1010 (1996); **54**, 2085 (1996).

[12] F. Šimkovic and A. Faessler, Few-Body Syst., Suppl. **9**, 231 (1996).

[13] M. Schepkin, Uppsala University Report No. TSL/ISV-96-01 41, 1996.

[14] I. T. Obukhovsky, V. G. Neudatchin, Yu. F. Smirnov, and Yu. M. Tchuvil'sky, Phys. Lett. **88B**, 231 (1979).

[15] M. Harvey, Nucl. Phys. **A352**, 301 (1981); **A352**, 326 (1981).

[16] Jin-Quan Chen, J. Math. Phys. **22**, 1 (1981); J. Q. Chen, *Group Representation Theory for Physicist* (World Scientific, Singapore, 1989); J. Q. Chen *et al.*, *Tables of the* $\mathrm{SU}(mn)\subset\mathrm{SU}(m)\times\mathrm{SU}(n)$ *Coefficients of Fractional Parentage* (World Scientific, Singapore, 1991).

[17] I. T. Obukhovsky, Yu. F. Smirnov, and Yu. F. Tchuvil'sky, J. Phys. A **15**, 7 (1982); I. T. Obukhovsky, Z. Phys. A **308**, 253 (1982); Prog. Part. Nucl. Phys. **36**, 359 (1996).

[18] V. G. Neudatchin, I. T. Obukhovsky, and Yu. F. Smirnov, Phys. Part. Nucl. **15**, 519 (1984).

[19] S. T. So and D. Strotmann, J. Math. Phys. **20**, 153 (1979).

[20] A. M. Kusainov, V. G. Neudatchin, and I. T. Obukhovsky, Phys. Rev. C **44**, 2343 (1991).

[21] A. Faessler, F. Fernandez, G. Lübeck, and K. Shimizu, Phys. Lett. **112B**, 201 (1982); Nucl. Phys. **A402**, 555 (1983).

[22] F. Tabakin, Phys. Rev. **174**, 1208 (1968).

[23] T. Ueda, K. Tada, and T. Kameyama, Prog. Theor. Phys. **95**, 115 (1996).

[24] O. F. Nemetz, V. G. Neudatchin, A. T. Rudchik, Yu. F. Smirnov, and Yu. F. Tchuvil'sky, *Nucleon Clusters in Atomic Nuclei and Many-Nucleon Transfer Reactions*, Monograph in Russian (Kiev, Naukova Dumka, 1988); V. G. Neudatchin, Yu. F. Smirnov, and N. F. Golovanova, Adv. Nucl. Phys. **11**, 1 (1978).

[25] M. Hamermesh, *Group Theory and its Application to Physical Problems* (Adison-Wesley, Reading, MA, 1964).

[26] S. Nakaishi-Maeda, Phys. Rev. C **51**, 1663 (1995).

[27] V. I. Kukulin, V. M. Krasnopol'sky, V. N. Pomerantzev, and B. P. Sazonov, Phys. Lett. **153B**, 7 (1985).

[28] A. Faessler, A. Buchmann, and Y. Yamauchi, Int. J. Mod. Phys. E **2**, 39 (1993).